Estimating heat fluxes and the Urban Heat Island (UHI) of Phoenix with remote sensing and meteorological data

Alexander Buyantuyev[1], Anthony Brazel[2], and Chris Eisinger[3]

[1]School of Life Sciences; [2]Department of Geography; [3]Mars Space Flight Facility, Department of Geological Sciences, Arizona State University, Tempe

INTRODUCTION

The urban heat island (UHI) effect is expressed in increased air and surface temperature in urbanized area compared to the countryside. It occurs as a result of increased sensible heat flux from land surfaces to the atmosphere near cities. Sensible heat flux consists of two components: discharged anthropogenic heat and heat radiation due to solar input. Heat from solar radiation is often enhanced by artificial land surfaces that are characterized by high heat capacities and conductivities. Another factor of UHI is the decrease in vegetation cover. Evapotranspiration associated with higher vegetation cover significantly reduces surface temperature. Understanding and quantifying UHI factors is an important step toward developing adequate mitigation strategies.

Two approaches to the analysis of UHI exist. In situ measurements by eddy covariance provide accurate determination of heat fluxes in urban environments at the roof-level (Arnfield, 2003; Oke et al., 1999; Taha, 1997). However this method is incapable of capturing the variety of land surfaces and spatial heterogeneity, even at the fine scale, of urban landscapes. Yet the spatial distribution of transpiration and surface heat fluxes can be estimated using remote sensing data coupled with local meteorological observations (Chrysoulakis, 2003; Kato & Yamaguchi, 2005; Schmugge et al., 1998). In this project we implement the method proposed by Schmugge et al. (1998) and Kato and Yamaguchi (2005) for estimating heat fluxes and separating the anthropogenically discharged heat and natural heat radiation from the sensible heat flux in urban areas by combining remote sensing and meteorological data.

REMOTE SENSING DATA

• We used cloud-free and atmospherically corrected ASTER (Advanced Spaceborne Thermal Emission and Reflection Radiometer) Level 1B and 2 data products of surface spectral reflectance, spectral emissivity, and surface temperature (Figure 1). Nominal ground spatial resolution is 15 m for the three Visible and Near-infrared, 30 m for six Shortwave, and 90 meters for five Thermal spectral channels. Narrow band spectral emissivities were converted to broadband emissivity using linear equation proposed by Ogawa et al (2003). This poster is based on the processed set of image products for night time (collected on June 21, 2003 at 9:40 pm MST).

• Landsat Enhanced Thematic Mapper (ETM+) image (30 m pixel) from May 2000 was used to create the land use – land cover map (Figure 2). Classification was performed using the expert system approach (Stefanov et al., 2001).

• 10-meter National elevation dataset (NED) Digital Elevation Model (DEM) by USGS and City of Phoenix street network layer were used as reference data and to model temperature gradients.

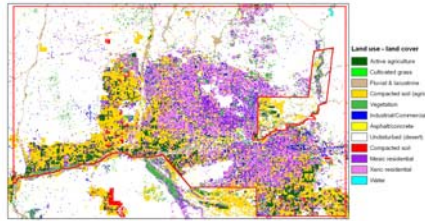**Figure 1**. Surface temperature from nighttime ASTER image (June 21, 2003, 9:40 pm MST)

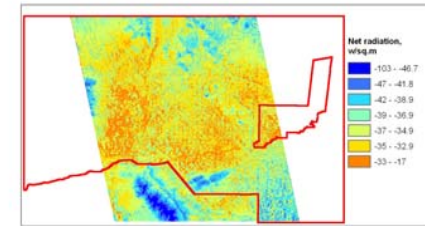**Figure 2**. Landsat ETM+ produced 12-class land cover classification of CAPLTER (Spring 2000)

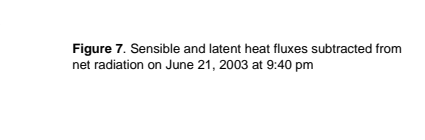**Figure 5**. Net radiation of the study area on June 21, 2003 at 9:40 pm

METEOROLOGICAL DATA

Meteorological data were obtained from five weather networks. Six variables - air temperature, wind speed, solar radiation, relative humidity, and air pressure recorded hourly/at 5 minute intervals - from a total of 67 stations were compiled into a single database. Observations closest in time to each of the ASTER images overpass were interpolated on a raster grid (Figure 3). Air temperature was gridded in two steps. First, actual observations were converted into hypothetical air temperature near land surface at 0 m above sea level (ASL) by applying a 6.5 K/km environmental lapse rate, which is the international standard set forth by the International Civil Aviation Organization (ICAO). Second, we used geostatistics and kriging interpolator to produce a horizontal temperature distribution at 0 ASL. Finally, the air temperature grid was created by using DEM and inverting the environmental lapse rate to the previously interpolated temperature surface. Relative humidity was interpolated by kriging without altitudinal correction because of the weakly localized distribution and smaller number of observations. Air pressure was calculated using hydrostatic equation. Vapor pressure was computed from relative humidity and saturation water vapor pressure which is obtained from the air temperature

ESTIMATION OF HEAT FLUXES

In the absence of advection or precipitation, the energy balance at the land surface is given by $R_n - G - LE - H = 0$ where R_n is the net radiation, G is the ground (soil) heat flux, LE is the latent heat or moisture flux into the atmosphere, and H is the sensible heat flux. Net radiation is calculated as the sum of incoming solar radiation and long-wave radiation emitted from the atmosphere to land surface and from the land surface to the atmosphere:

$$R_n = (1 - \alpha) R_s + \varepsilon\varepsilon_a \sigma T^4 \downarrow + \varepsilon \sigma T^4 \uparrow$$

where R_s is the short-wave radiation, $\sigma T4$ is the downward ($\downarrow$) and upward ($\uparrow$) blackbody radiation described by the Stefan-Bolzmann Law (W/m2), σ is the Stefan-Bolzmann constant, T is surface temperature, α is the surface albedo, ε is the surface emissivity and εa is the atmospheric emissivity. ε_a is calculated based on the following empirical equation (Brutsaert, 1982): $\varepsilon_a = 1.24(e_a/T_a)^{1/7}$, where e_a is the atmospheric water vapor pressure in hPa and T_a is the atmospheric temperature.

G was estimated as the fraction of R_n using fixed coefficients for each surface type based on empirical relationship.

Sensible and latent heat fluxes were obtained using the bulk resistance approach. The sensible heat flux into the atmosphere is:

$$H = \rho C_p \frac{T_s - T_a}{r_a}$$

where ρ is the air density, C_p is the specific heat of air at constant pressure in J/kgK, T_s is the surface temperature, and r_a is the aerodynamic resistance in s/m. C_p is corrected based on air pressure and vapor pressure. The r_a is rather complex function of various physical parameters of land surfaces and the wind speed and is usually determined empirically (Brutsaert, 1982).

Latent heat flux is expressed as

$$LE = \frac{\rho C_p (e_s^* - e_a)}{\gamma (r_a - r_s)}$$

where γ is the psychrometric constant, is the saturation vapor pressure (hPa) at the surface temperature. r_S is the stomatal resistance (s/m) whose value depends on vegetation, meteorological and atmospheric conditions

In urban areas in addition to the net radiation the anthropogenic heat discharge also causes heat fluxes. Human activities, mainly energy production, use of machinery, air conditioning, and automobiles generate additional ground, sensible, and latent heat fluxes (Fig. 4). This can be described by modifying the heat balance equation as follows:

$$Rn - G - LE - H = 0$$

where A is the total anthropogenic discharge. A here represents energy transformed 1) into latent heat via phase changes of water due to power generation and the generation and supply of hot water; 2) as sensible heat transferred into the atmosphere as heated gas from outdoor air conditioning units, through chimneys etc. In addition anthropogenic sensible heat contributes to increased surface temperature. It is possible to estimate the effect of anthropogenic heat on heat balance by first calculating all the heat fluxes and than inferring the artificially created heat (Kato & Yamaguchi, 2005). Sensible heat flux estimation implies a composite of consequences from radiant heat balance and the effect of anthropogenic heat discharge because it is calculated based on observed surface and air temperatures. In contrast, the latent heat flux is calculated for the evapotranspiration without consideration of anthropogenic factor. The net radiation depends on long-wave radiation which is a function of surface and air temperatures. However this influence is sufficiently small compared to the solar radiation under clear skies during daytime. The effect of temperature change on G is small. All the above considerations let one to conclude that the influence of temperature rise on heat flux is negligible, with the exception of sensible heat. The surplus in the radiant heat balance can thus be attributed to the anthropogenic effects. All the above considerations let one to conclude that the influence of temperature rise on heat flux is negligible, with the exception of sensible heat. The surplus in the radiant heat balance can thus be attributed to the anthropogenic effects. The sensible heat flux due to radiant heat balance (Hn) can be defined as the residue of the heat-balance equation: $Hn = Rn - G - LE$. The sensible heat flux due to anthropogenic effects can then be calculated as $H_{as} = H - Hn$. where H_{as} is the net increase in sensible heat flux given by the surface heat balance and is not equivalent to A.
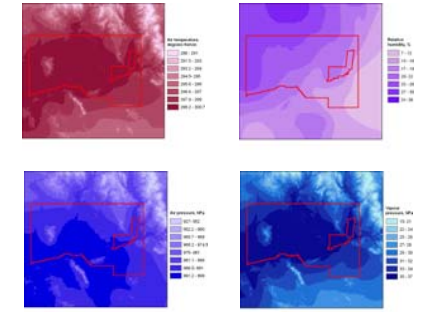

Figure 3. Atmospheric temperature corrected by DEM, relative humidity, air pressure inferred from hydrostatic equation, and atmospheric vapor pressure interpolated for the study area (June 21, 2003 @ 9:40 pm). CAPLTER boundary is in red.
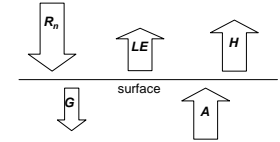

Figure 4. Schematic diagram of heat balance at urban land surface. Rn is net radiation, A – anthropogenic heat discharge, G – ground heat flux, LE – latent heat flux, and H – sensible heat flux (redrawn from (Kato & Yamaguchi, 2005))
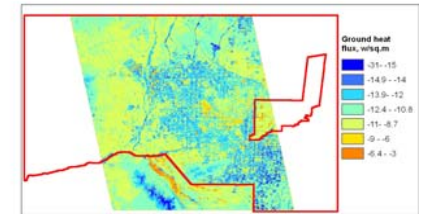

Figure 6. Ground heat flux of the study area on June 21, 2003 at 9:40 pm

PRELIMINARY RESULTS AND FUTURE WORK

Spatial distribution of summer nighttime net radiation shows strong dependence on the urban landscape pattern. It is generally higher in the urban core and along transportation network, and it decreases with elevation and away from the built-up areas. Some natural areas with exposed bedrock and agricultural fields also have higher net radiation. Ground heat flux (Figure 6) is inversely related to the urban spatial pattern by being the lowest in urbanized area characterized by high degree of impervious surfaces such as pavements, buildings etc. The sensible heat flux due to anthropogenic factors (Has) cannot be computed with sufficient accuracy for nighttime due to the absence of solar radiation which causes the effect of relative increase of air and surface temperatures on heat fluxes. Kato and Yamaguchi (2005) used H in place of the H_{as} for their nighttime data stating that no sensible heat flux was discharged from most of their study area except in the urban, industrial areas, and water. They found that the spatial distribution of H_{as} in the daytime correlated well with the urbanized areas where energy consumption is the highest. Figure 7 illustrates the combined effect of the two fluxes (H and LE) derived by a simple subtraction of G from the net radiation. Since dry built-up portion of the urban landscape does not have any latent heat flux most of the increased heat can be attributed to the sensible heat flux. Preliminary analysis has shown negligible sensible heat flux calculated by the equation, which allows us to conclude that most of the increased heat in the urban area as shown on the map (Figure 7) is H_{as}.

Figure 7. Sensible and latent heat fluxes subtracted from net radiation on June 21, 2003 at 9:40 pm